Mixed crystals in chiral organic systems: phase diagram and crystal structure features of an ethanolamine salt of 3-chloromandelic acid

9 AUTHORS, INCLUDING:

Valérie Dupray

Université de Rouen

37 PUBLICATIONS **224** CITATIONS

SEE PROFILE

Gérard Coquerel

Université de Rouen

197 PUBLICATIONS **1,529** CITATIONS

SEE PROFILE

CRYSTAL GROWTH & DESIGN

Article

pubs.acs.org/crystal

Mixed Crystals in Chiral Organic Systems: A Case Study on (*R*)- and (*S*)-Ethanolammonium 3-Chloromandelate

N. V. Taratin,*[,†] H. Lorenz,[‡] E. N. Kotelnikova,[†] A. E. Glikin,[†,¶] A. Galland,[§] V. Dupray,[§] G. Coquerel,[§] and A. Seidel-Morgenstern[‡]

[†]Saint-Petersburg State University, Crystallography Dept., St. Petersburg, 199034, Russia

[‡]Max Planck Institute for Dynamics of Complex Technical Systems, Magdeburg, 39106, Germany

[§]Rouen University, SMS Laboratory, UPRES EA 3233, IRCOF, Mont-Saint-Aignan Cedex, 76821, France

Supporting Information

ABSTRACT: This work focuses on characterization of chiral organic systems with partial solid solutions. Particularly, behavior of the (*R*)- and (*S*)-ethanolammonium 3-chloromandelates (E3ClMA) has been investigated experimentally. Partial solid solutions of the series (*R*)-E3ClMA−(Rac)-E3ClMA and (*S*)-E3ClMA−(Rac)-E3ClMA were discovered at the eutectic type of the binary phase diagram by means of systematic differential scanning calorimetry and X-ray powder diffraction measurements. Solubility and metastable zone width were measured for solutions of (*R*)-E3ClMA, (Rac)-E3ClMA, and their mixtures in ethanol as the solvent. The crystal structure of the pure (*R*)-E3ClMA was successfully determined by single-crystal X-ray diffraction. Several efforts of single crystals productions from (*R*, *S*) solutions were made by means of cooling and evaporation methods. Crystal morphology changes from well-shaped crystals for the pure enantiomer to spherulites for the racemic composition.

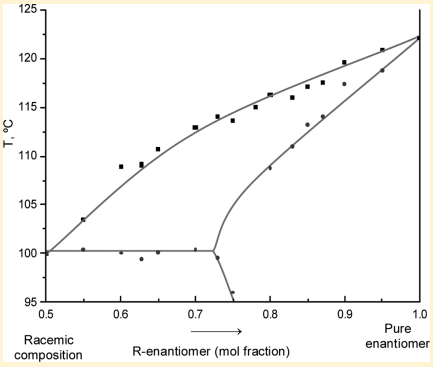

1. INTRODUCTION

Mixed crystals (solid solutions, isomorphic mixtures) occur quite often in organic and inorganic systems as well as they present a majority of natural minerals. Understanding of mixed crystal formation processes has become an object of special scientific interest in different fields due to a feasible creation of smart materials with predetermined properties and elaboration of new approaches to mineral genesis reconstructions. Crystal chemistry and thermodynamics of solid solutions were successfully developed during the 20th century, especially for inorganic substances in frames of metallurgy and mineralogy.[1,2] Some concepts for organic mixed crystals were also elaborated.[1,3−5] During the last 30 years,[6] the genetic concept was established for mixed crystals.[7] However, a comprehensive theory of mixed crystal formation, which could be applied for a priori design of mixed crystal properties, is not elaborated yet.

A pair of enantiomers represents molecules of mirror antipodes. The molecules have identical physical properties (apart from opposite optical rotation) but cause different effects on biological systems. Therefore, the enantiomeric purity of a material plays an essential role in the pharmaceutical and food industry. An equimolar mixture of two antipodes produces an optically inactive solution. The substance crystallized from such a solution is called a racemate. Composition ranges of "(*R*)-enantiomer−racemic composition" and "(*S*)-enantiomer−racemic composition" are equal due to the mirror symmetry of the corresponding phase diagrams.[8] The type of phase diagram is related to the nature of a racemate. A mechanical mixture of enantiomers refers to a racemic conglomerate and corresponds to a eutectic system. Structural ordering of enantiomers inside a crystal corresponds to a racemic compound and occurs in a congruent melting system. Continuous solid solutions in chiral organic systems are a rare case (~1%). Furthermore, partial solid solutions of enantiomers in eutectic and congruent melting systems occur much more often than expected in the past; some examples were described in the literature recently.[9−12]

This work focuses on verification and characterization of partial solid solutions of the (*S*)- and (*R*)-enantiomers of the ethanolamine salt of 3-chloromandelic acid (E3ClMA, Figure 1). This research originates from a comparison between E3ClMA with the ethanolammonium mandelate, which forms

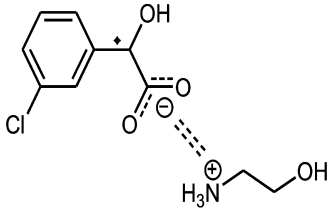

Figure 1. Ethanolamine salt of 3-chloromandelic (E3ClMA). Position of the chiral center is marked by the dot.

Received: March 12, 2012
Revised: October 23, 2012
Published: October 24, 2012

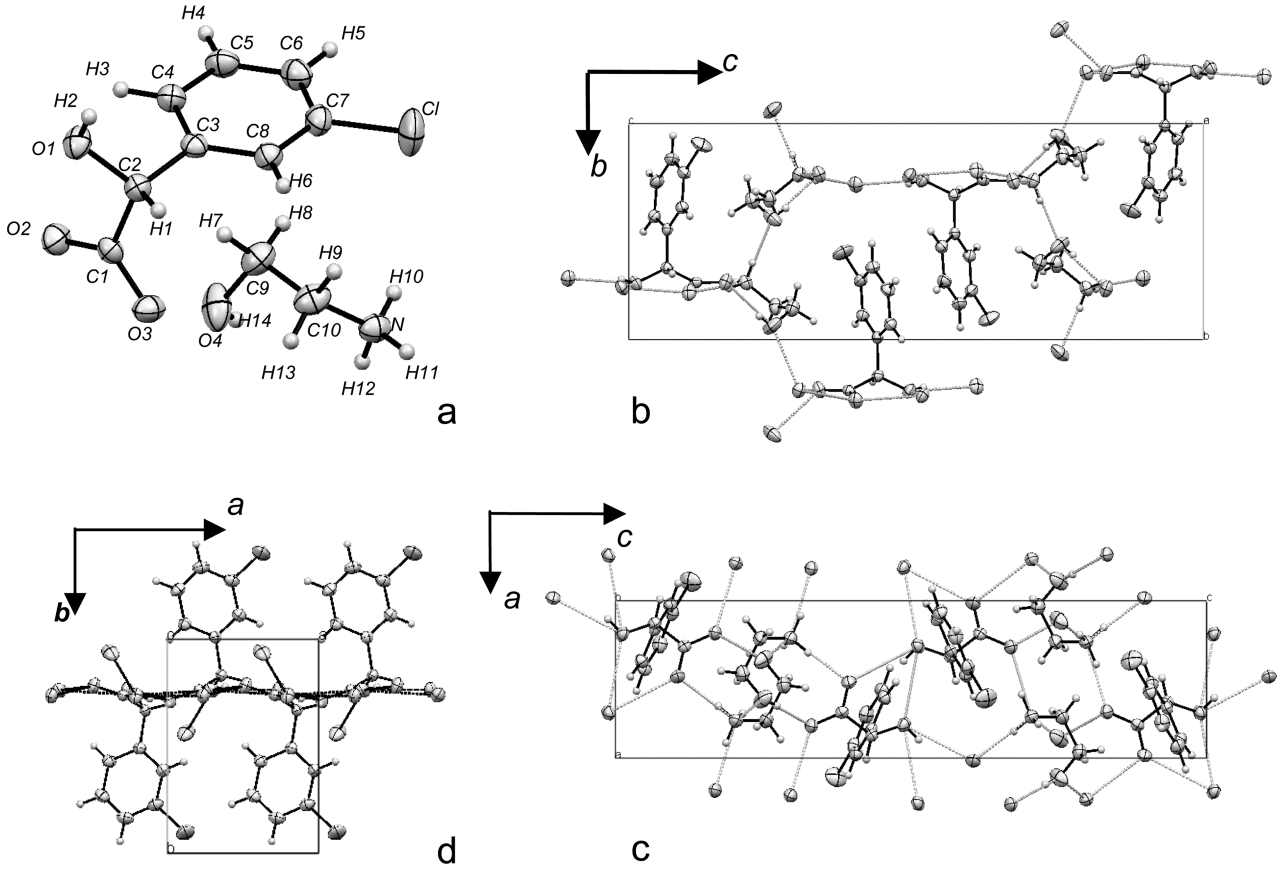

Figure 2. (a) 3-Chloromandelate (top) and ethanolammonium (bottom); (b–d) projections of the crystal structure onto planes bc (b), ac (c), ab (d).

a stable conglomerate with partial solid solutions.[10] Indeed, the substances could be expected to form another conglomerate with possible partial solid solutions, since a preliminary test has shown a positive second harmonic effect in nonlinear optics.[13]

In a first step, the crystal structure of the pure (*R*)-E3ClMA was successfully solved and refined by means of direct methods. The binary phase diagram of the E3ClMA system was determined by means of systematic differential scanning calorimetry (DSC) and X-ray powder diffraction (XRPD) measurements. Crystal lattice parameters were calculated for mixtures with different enantiomeric ratio. In a second step, solubility in ethanol and metastable zone width data (MZW) were measured as functions of the mixture composition. Solid–liquid equilibria were estimated in ethanol at 30 °C. Finally, several efforts were made to grow single crystals from aqueous solutions to evaluate crystal morphology.

2. EXPERIMENTAL SECTION

2.1. Substances. (*R*)-enantiomer [(*R*)-E3ClMA)] and the racemic mixture [(Rac)-E3ClMA)] of the ethanolamine salts of 3-chloromandelic acid were used as initial substances. All batches of substances were produced using 3-chloromandelic acid and ethanolamine (by Aldrich and Alfa Aesar, respectively) in the same way as follows. A solution of 3-chloromandelic acid was prepared first. Then, while stirring, a stoichiometric mass of pure ethanolamine (liquid state under normal conditions) was added, which provoked spontaneous crystallization of the salt after a few minutes. Finally, the slurry was filtered off and dried. The ethanol–water azeotropic mixture, (95.57% of ethanol, "ethanol" throughout the text) was used as solvent in investigation of the ternary system.

2.2. Determination of the (*R*)-E3ClMA Crystal Structure. The crystal structure of the pure (*R*)-E3ClMA was determined by single-crystal X-ray diffraction (IPDC II, STOE). The structure was solved by means of direct methods and refined with SHELX97 software.[14] The single crystal growing procedure is explained in detail in Section 2.5.

2.3. Determination of the Binary Phase Diagram: DSC and XRPD Analyses. A comprehensive range of the phase diagram between (*R*)- and (Rac)-E3ClMA was investigated; the range between the (*S*)-enantiomer and the racemic mixture was constructed as the symmetrical image. Different amounts of (*R*)- and (Rac)-E3ClMA were weighted (errors <0.1 wt %) to prepare samples with compositions, which were determined as a part of the (*R*)-enantiomer in the (*R*)-(*S*)-mixture. A sufficient amount of ethanol was added, and the sample was stirred until dissolution occurred. Samples were dried at room temperature and crushed in a mortar. The average weight typical for the sample was about 50 mg. Each sample was split for DSC (DSC 131, SETARAM, France, closed aluminum crucibles, 10–12 mg of substances sample, heating rate 1 K/min) and XRPD (X' Pert Pro Diffractometer, PANanalytical GmbH; X'Celerator detector, Cu Kα radiation, 2Θ range 3–40°, 300 s/step, 2Θ step 0.004°).

Melting temperatures of (*R*)- and (Rac)-E3ClMA were taken from extrapolated DSC-onset temperatures within the heat flux/temperature plot. The initial stage of the melting was correlated by extrapolation of the appropriate onset temperature in the cases of mixtures. The liquidus line for mixtures was correlated by extrapolation to the top of peak value. The heat of fusion values (J/mol) were also calculated.

The internal reference of sodium chloride (~10 wt %) was used to avoid any zero shift in the XRPD measurements. Initial positions of 2Θ and intensities were accurately determined by means of the profile fitting in the X'Pert High Score Plus software. After this, positions of 2Θ were shifted according to the constant systematic correction, and

dx.doi.org/10.1021/cg3003405 | *Cryst. Growth Des.* 2012, 12, 5882–5888

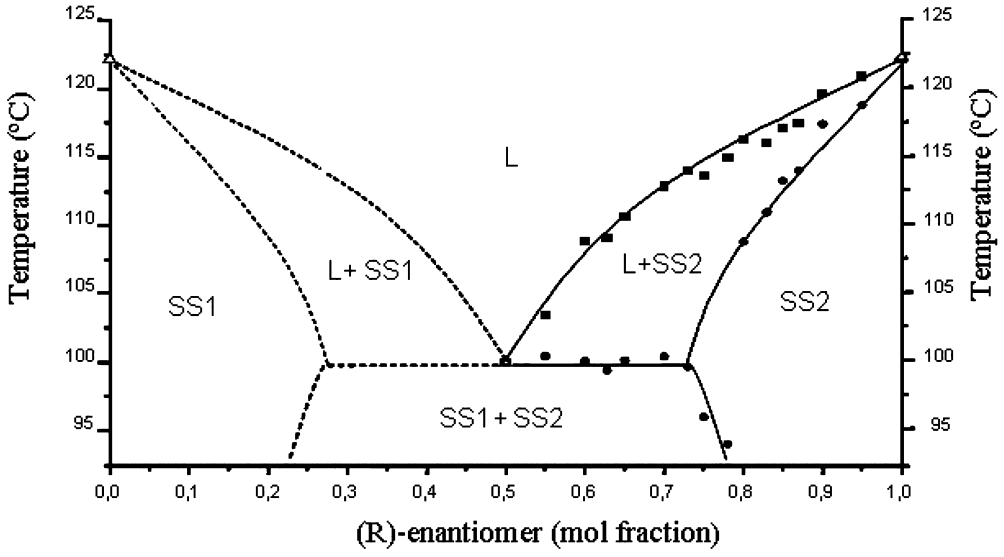

Figure 3. Binary phase diagram of the E3ClMA system.

peaks of XRPD patterns were indexed. The identical set of 18 peaks was used for unit cell calculations for all samples.

2.4. Measurements of Solubility, MZW, and Estimation of Solid–Liquid Equilibrium Compositions. The solubility in ethanol was measured by means of polythermal and isothermal methods.[15]

The Crystal16 multiple-reactor system (Avantium Technologies, The Netherlands) was used for polythermal determination of solubilities within the temperature range of 20–40 °C. Compositions from the pure enantiomer to the racemic mixture with 10% composition steps were investigated. Samples were dissolved in ethanol and put in the Crystal16 multiple-reactor system. Quick change of the solution temperature in the experiment was assured using a small vial volume (1 mL) and continuous stirring. Changes of slurry transparency during cooling or heating (with 0.05 K/min rate) were detected. A cloudy solution with minimal transparency indicates the crystallization of the sample; oppositely, a transparent solution corresponds to the dissolution of the sample. The temperature of the total dissolution of the slurry was correlated with the saturation of the solution with given concentration. The MZW was determined as a difference between temperature of transparent and cloudy solutions.

In the case of the isothermal method, a defined amount (mg) of the pure enantiomer and the racemate was put into a sealed vial and mixed with 5 mL of ethanol. The prepared slurry was continuously stirred and thermostatted at 30 °C for two weeks. We applied the isothermal method not only for additional measurements of solubilities but rather for the estimation of compositions of solid and liquid phases in equilibrium. The equilibrated liquid and solid phases were carefully separated, and then, the solid was dissolved in acetone. Both solutions were analyzed by chiral high-performance liquid chromatography (HPLC), using the following conditions: analytical column Chirobiotic T, 5 μm, 1% TEAA/MeOH (80/20) at pH 4.02; V_{eluent} = 0.5 mL/min.

2.5. Preparation of Single Crystals. Much effort was put on single crystal production by means of either cooling or evaporation of solutions of the pure enantiomer and intermediate enantiomer–racemate compositions. Crystals of the pure enantiomer were used for single crystal X-ray diffractometry as well as for observations of their morphologies and imperfections by means of optical microscopy.

In the case of cooling crystallization, (*R*)-E3ClMA was dissolved in ethanol with a final concentration of 50 g/L and put into a sealed vial thermostatted at 30 °C for few days. Then, the temperature was stepwise gradually reduced to 5 °C. In the case of evaporation crystallization, solutions of pure (*R*)-E3ClMA with different concentrations in 10 mL of ethanol were filled in a Petri dish and placed under an exhaust hood at room temperature until crystals appeared and reached needed sizes. Crystals grown from solutions with a different ratio of both enantiomers were produced in the similar way but also from aqueous solutions.

3. RESULTS AND DISCUSSION

3.1. Crystal Structure of Pure (*R*)-E3ClMA. The crystal structure of pure (*R*)-enantiomer was resolved in the widespread chiral space group $P2_12_12_1$ (Z = 4) with the following lattice parameters: a = 5.953(3) Å; b = 8.396(1) Å; c = 22.37(11) Å at room temperature. The final cycle of full-matrix least-squares refinement on F^2 led to $R1/wR2$ = 0.0440/0.0948 and goodness-of-fit = 1.031 for all 3021 data. Non-hydrogen atoms were refined with anisotropic displacement parameters, and hydrogen atoms were refined with isotropic displacement parameters.

The crystal structure of (*R*)-E3ClMA presents the alternate of nonchiral ethanolammonium and chiral 3-chloromandelate layers (Figure 2), interconnected by hydrogen bonds. Ethanolammonium is connected by N–H11···O4 (length 1.87 Å) bonding; 3-chloromandelates are connected by O1–H2···O3 (length 2.19 Å) and O1–H2···O1 (length 2.19 Å), involving the chiral center. Moreover, each carboxyl group of 3-chloromandelate is interconnected with two ethanolammoniums by three hydrogen bonds (O4–H14···O2, N–H12···O3, and N–H11···O2 with lengths of 1.87, 1.93, and 1.87 Å, respectively).

As it was mentioned above, E3ClMA has a similar stereochemistry to the ethanolammonium mandelate ((*R*)-EMA).[10] The crystal structure of (*R*)-E3ClMA has the same space group, the same conformation, and a similar hydrogen-bond network as (*R*)-EMA. Consistently, the chlorine atom of E3ClMA is not involved in any hydrogen bond: the distance between the chlorine atom and the nearest hydrogen atom (H13) is 2.84 Å and therefore too long compared with usual hydrogen bonds (1.87–2.19 Å).

3.2. Binary Phase Equilibria. *3.2.1. DSC Data.* Only endothermic effects caused by substance melting were recorded by means of DSC analysis. DSC measurements of pure (*R*)- and (Rac)-E3ClMA, which are presented each by a single melting peak, reveal melting at 123 and 100 °C and specific melting enthalpies of 47.4 and 34 kJ/mol, respectively.

dx.doi.org/10.1021/cg3003405 | *Cryst. Growth Des.* 2012, 12, 5882–5888

The binary phase diagram of the (*R*)- and (*S*)-E3ClMA system presents an eutectic invariant with partial solid solutions (Figure 3). Two main regions can be pointed out on this plot.

The areas from 0.8(*S*)-E3ClMA up to pure (*S*)-E3ClMA and from 0.8(*R*)-E3ClMA up to pure (*R*)-E3ClMA correspond to symmetrical partial solid solutions labeled as SS1 and SS2 in Figure 3. This is confirmed by a single broad peak on DSC curves in this range of compositions.

The region of 0.8(*S*)-E3ClMA−0.8(*R*)-E3ClMA corresponds to the miscibility gap of the solid solutions. All samples, which belong to the nonmiscibility area, should be expressed as a mixture of coexistent solid solutions SS1 and SS2 (Figure 3) below approximately 100 °C. Compositions of these solid solutions should correspond to the miscibility limits of the solid solution.

The exact miscibility boarders could not be determined from DSC curves alone. The last clear eutectic peak was observed for the 0.74(*R*)-E3ClMA mixtures (Figure 3). Therefore, the Tammann plot was constructed by plotting the eutectic part of the heat of fusion ($\Delta_f H_{eutec}$) as a function of composition (Figure 4). Calculated values of eutectic heat of fusion were

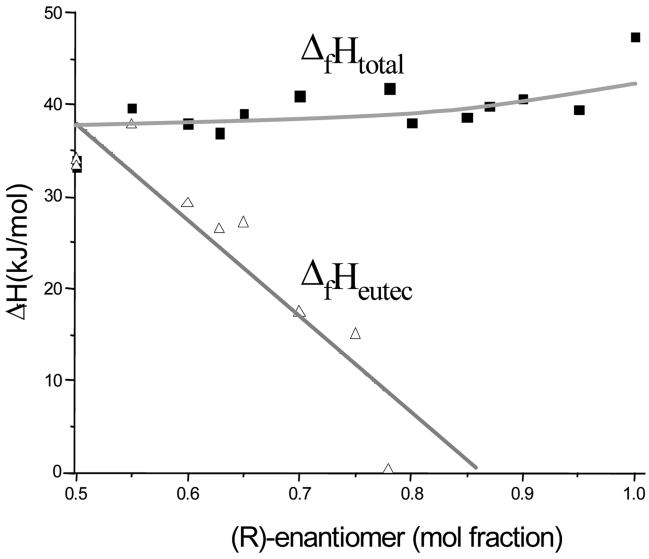

Figure 4. Tammann plot of the total and eutectic heats of fusion.

approximated linearly. The straight line for $\Delta_f H_{eutec}$ (R^2 = 80%) intersects with the composition axis at about 0.85(*R*)-E3ClMA. The deviations observed might be due to an uncompleted disintegration of the initial samples into eutectic solid solutions and therefore changes of the miscibility boarder position from sample to sample.

3.2.2. XRPD Data. XRPD patterns are similar for the pure enantiomer samples and intermediate compositions and characterized by a small 2Θ shift of some peaks. They showed that all crystals belong to orthorhombic symmetry ($P2_12_12_1$ space group).

The shift of lattice parameters is minimal for *a* (0.03 Å, Figure 5a), intermediate for *b* (∼0.06 Å, Figure 5b), and maximal for *c* (∼0.10 Å, Figure 5c); the respective cell volume change is about 13 Å^3 at its maximum (Figure 5d). The unit cell volume increases with incorporation of the counter-enantiomer; the same trend characterizes shifts of *b* and *a* parameters, but the shift of *c* is opposite. Significant changes of crystal lattice parameters with the incorporation of the counter-enantiomer appear in the range from pure (*R*)-E3ClMA to about 0.75(*R*)-E3ClMA and therefore confirm the existence of solid solutions (Figure 5a−d). Further enrichment of the initial solution with the counter-enantiomer results in an almost constant value of lattice parameters of the precipitated solid (Figure 5a−d, range from the racemic composition to about 0.75(*R*)-E3ClMA). This corresponds to crystals with a similar composition and characterizes the area of nonmiscibility of solid solutions. Significant deviations of lattice parameters from the plotted trends relate to the broadening of some XRPD peaks of corresponding samples and therefore coordinated in an inaccuracy of the determination of peak position. Possible reasons of such broadening[16] are as follows: the decrease of crystal domain size, the increase of intercrystal stresses, or inhomogeneities in crystal compositions.

Obviously, the increase of the unit cell volume from the pure enantiomer to the racemic mixture points up the distortion of the structure concomitant with the substitution of the counter-enantiomer and corresponds to the decrease of the close packing of molecules in the crystal structure. Volumes of molecules of enantiomers are the same. Therefore, the increase of the unit cell volume in the case of (*R*, *S*) solid solutions should be related to the rearrangement of hydrogen bonds (especially around the "chiral" hydrogen bond O1−H2···O3) and to the changes of the intermolecular contacts inside the crystal structure.

3.3. Solubility, MZW, and Estimation of Solid−Liquid Equilibrium Compositions. Results of polythermal solubility measurements in ethanol are presented as solution concentration versus saturation temperature (Figure 6). In the 20−40 °C studied temperature range, the solubility shows a nonlinear increase for mixtures with constant compositions.

These data were used for construction of the Lippmann diagram adapted for soluble compounds by Treivus[17] (Figure 7). It reveals an increase in the solubility with addition of the opposite enantiomer, which is a typical situation for conglomerate-type enantiomeric systems.[8] However, nonlinearity of the solubility isotherms points out the nonideal behavior of the E3ClMA system.

The solidus curve (equilibrium solid compositions) cannot be determined from polythermal data. However, solid−liquid equilibria were estimated from the results of isothermal experiments (Figure 8). Compositions of the initial solutions and the equilibrated solids are different, which confirms solid solutions. The increase of the compositional difference between equilibrated solid and liquid phases from the pure enantiomer to the racemic composition marks the miscibility gap. Only a general trend could be derived from the measurements, since some uncertainties affect the determination of equilibrated solid−liquid compositions as follows. First, HPLC provides the overall composition of a solid sample, which is a mixture of two solid solutions in the case of the eutectic area. For this reason, the equilibrated solid phase of the racemic mixture has a composition 0.5(*R*)-E3ClMA that corresponds to the equimolar mixture of solid solutions of symmetrical compositions. Second, the equilibration process can take a long time in the case of solid solutions due to blocking of the crystal surface with the isomorphic phase during a reaction between crystals and solution components (such effects were determined for inorganic systems[6,7]).

To complete solubility analysis, we have focused our attention on metastable equilibria (Figure 9). The MZW increases with the addition of the counter-enantiomer to the

dx.doi.org/10.1021/cg3003405 | *Cryst. Growth Des.* 2012, 12, 5882−5888

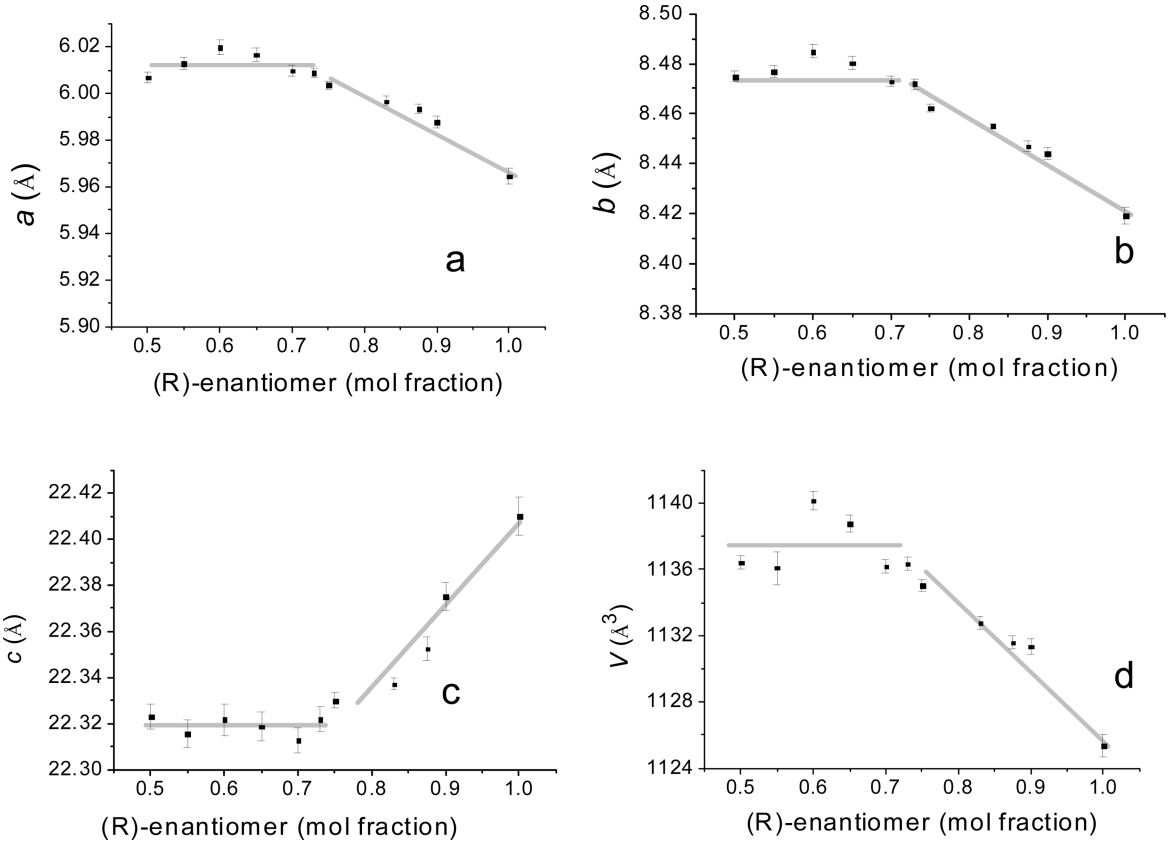

Figure 5. Dependence of lattice parameters on the sample composition.

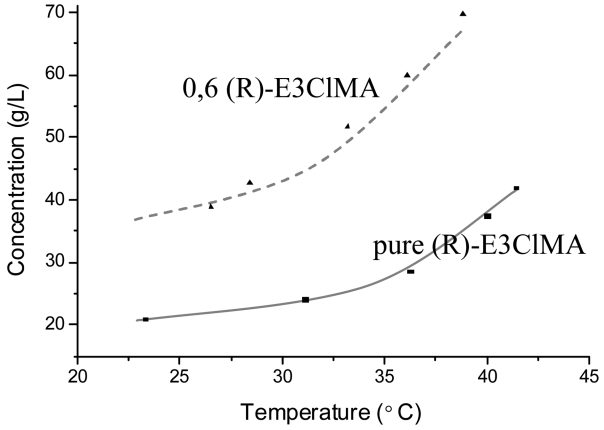

Figure 6. Solubility of pure (*R*)-E3ClMA and a 0.6(*R*)-E3ClMA mixture in ethanol.

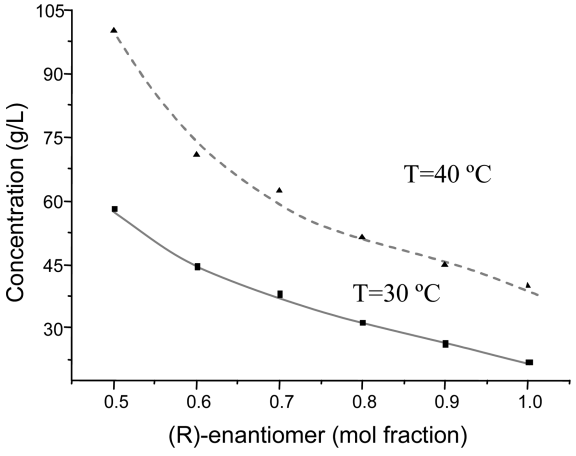

Figure 7. Solubility isotherms of (*R*)−(Rac)-E3ClMA mixtures in ethanol.

pure (*R*)-E3ClMA but does not change in the eutectic area. The minimum width of <23 K corresponds to the pure enantiomer and reaches a value of about 30 K with enrichment of the mixture with the counter-enantiomer (Figure 9).

3.4. Crystal Morphology. Single crystals of pure (*R*)-E3ClMA (size 4−7 mm) were successfully grown by means of evaporation from aqueous solutions. It should be noted that efforts for single crystal production by means of cooling were not successful: only gelation of the solutions without any crystallization was observed at maximum supercooling. The optimal concentration of solutions of pure (*R*)-E3ClMA in water was 450 g/L in the case of the evaporation methods. In order to adjust the optimal concentration of (*R*, *S*) solutions, the similarity of solubility trends in ethanol and water was hypothesized.

Results of single crystal growth experiments (Figure 10a−d) show a significant influence of the presence of the counter-enantiomer in the (*R*)-E3ClMA solution on crystal morphology. Crystals of pure (*R*)-E3ClMA are well shaped (Figure 10a). Addition of 10% (*S*)-E3ClMA changes drastically the crystal habit to needlelike crystals and causes multiheaded growth, which could be a first step of the skeletal growth,[18] or formation of excrescences of isomorphic reaction[6] (Figure 10b). Addition of more (*S*)-E3ClMA causes splitting (Figure 10c) up to the formation of spherulithes from the solution of racemic composition (Figure 10d).

dx.doi.org/10.1021/cg3003405 | *Cryst. Growth Des.* 2012, 12, 5882−5888

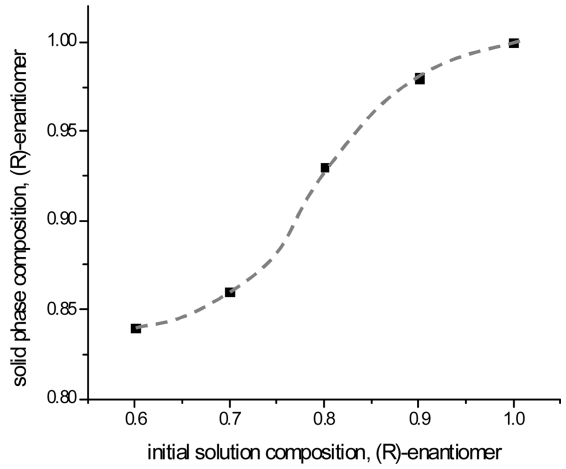

Figure 8. Estimated solid−liquid equilibria of E3ClMA in ethanol.

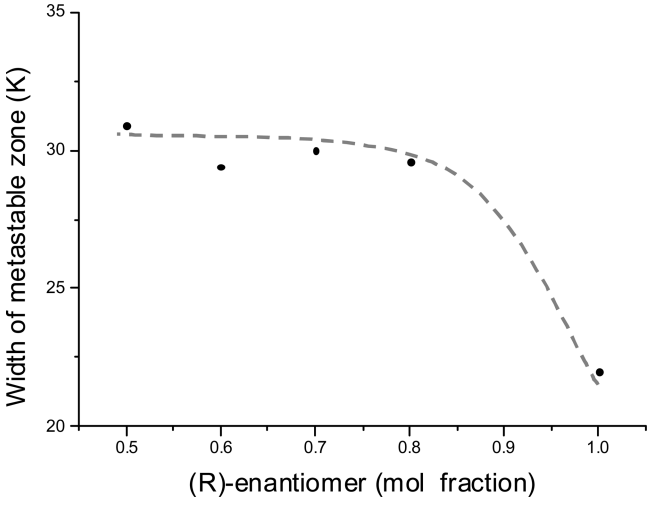

Figure 9. MZW of E3ClMA in ethanol versus a (*R*)-(Rac)-mixture composition.

Formation of splitted and spherulithic forms (Figure 10c, d) is usually related to a high supersaturation.[18] In the case of crystallization from (*R*, *S*)-E3ClMA solutions, the detected broad metastable zone (about 30 °C, Figure 9) could cause a high initial supersaturation at the spontaneous crystallization and promote splitting of the crystals. Furthermore, inhibition of crystal growth in a particular direction by tailor-made additives[5] could also influence the morphology of (*R*, *S*)-E3ClMA crystals.

The isomorphic exchange may cause also some morphological features accompanying growth processes.[7] The exchange reaction accompanies any growth process and consists in nonadequate changes of isomorphic compositions of solid and liquid phases (for example, due to local entrainment effect). As a result, isomorphic excrescences cover the crystal, forming either spongy or blocking patterns. Such phenomena were revealed using several inorganic systems and a metal−organic one.[6,7] Spongy patterns were also revealed for the chiral system: (+)- and (−)-methyl 2-(diphenylmethylsulfinyl) acetate.[12] Elements of multiheaded growth pointed out for 0.9(*R*)-E3ClMA (Figure 10b) might be blocking excrescences.

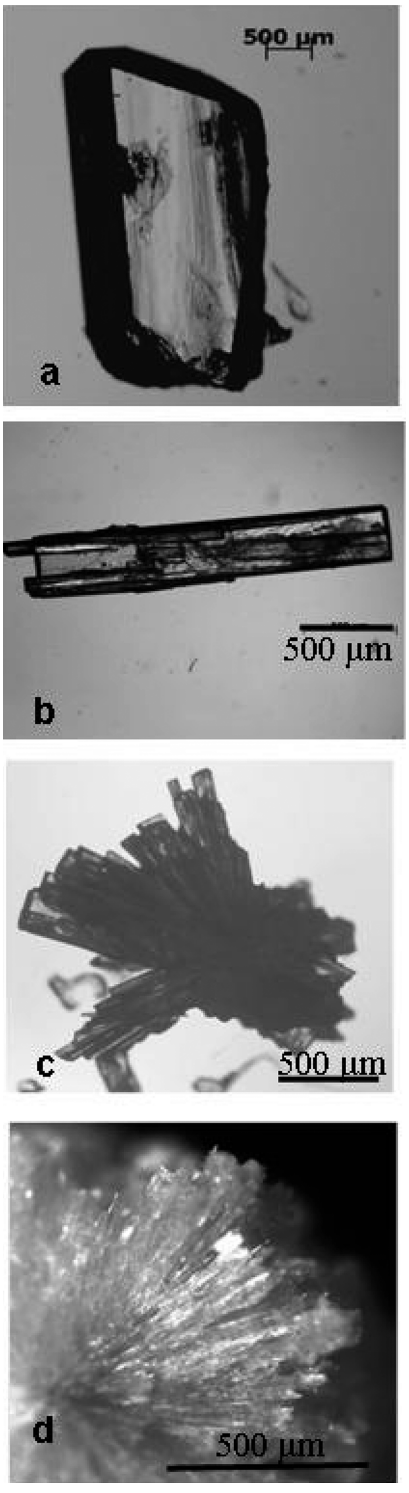

Figure 10. Morphology of crystals, grown from solution with different (*R*)/(*S*) enantiomer ratios. Composition and initial concentration of solutions: (a) pure (*R*)-E3ClMA, 450 g/L; (b) 0.9(*R*)-E3ClMA, 540 g/L; (c) 0.75(*R*)-E3ClMA, 670 g/L; (d) 0.5(*R*)-E3ClMA, 1000 g/L.

4. SUMMARY

Partial solid solutions of enantiomers were discovered in the conglomerate forming system: (*R*)- and (*S*)-ethanolammonium 3-chloromandelate. The domains in composition of the partial solid solutions and the corresponding nonmiscibility region were determined by using DSC and by calculations of crystal lattice parameters versus the enantiomeric excess. A good

dx.doi.org/10.1021/cg3003405 | *Cryst. Growth Des.* 2012, 12, 5882−5888

agreement between these two independent techniques has been obtained.

At a constant temperature, solubility increases in a nonlinear way from the pure enantiomer to the racemic composition and does not allow recognizing partial solid solutions directly. By contrast, the MZW increases with the addition of the counter-enantiomer to the initial mixture but does not change in the eutectic area. The estimated boundary composition between those two regimes is consistent with the binary and ternary phase diagrams.

Existence and absence of solid solutions should be related to crystal structure features. General relations between solubility in the solid state and crystal structure features were established by Kitaigorodskii.[1] Changeability of close packing of molecules inside the crystal structure and unbreakability of hydrogen bonds play an essential role in formation of solid solutions. In the case of E3ClMA, deterioration of close packing and possible rearrangement of hydrogen bonds promote the decay of solid solutions and the formation of the miscibility gap in the solid state.

Interestingly, the binary phase diagram and the crystal structure of the ethanolammonium 3-chloromandelate are similar to that of the ethanolammonium mandelate described previously.[10] This seems to be related to the absence of an H-bond involving the chlorine atom. It is worth noting that those similarities do not hold for the ethanolammonium 2- and 4-chloromandelates.

Extended similarities between ethanolammonium 3-chloromandelate and ethanolammonium mandelate have also been pointed out on morphological changes from well-shaped crystals for the pure enantiomer to spherulithes for the racemic composition making it difficult to access single crystals containing a significant amount of counter-enantiomer. This could be related to an increase of the MZW and/or some changes of crystal structure features coordinated with the inhibition of crystal growth in a particular direction during the incorporation of the counter-enantiomer.

■ ASSOCIATED CONTENT

Ⓢ Supporting Information

The crystal structure of (*R*)-E3ClMA as a CIF file. This material is available free of charge via the Internet at http://pubs.acs.org.

■ AUTHOR INFORMATION

Corresponding Author

*Phone/fax: +7(812)3289650; e-mail: crystal-lab-workshop@yandex.ru.

Notes

The authors declare no competing financial interest.

■ ACKNOWLEDGMENTS

This research was done in the frame of a Russian President Grant for abroad education, supported by the RFBR grants (12-05-00876, 10-02-01303, and 10-05-00891) and the Russian President grant for young Doctors of Science (no. 442.2009.5). The authors thank Dr. Jan von Langermann (MPI Magdeburg) for advices in the synthesis of initial substances.

■ DEDICATION

¶Arkady Glikin passed away just before the final print of this article, which he essentially initiated and shaped.

■ REFERENCES

(1) Kitaigorodskii, A. *Mixed Crystals*; Springer: New York, 1984.
(2) Urusov, V. S. *Theoretical Crystallochemistry*; Moscow State University Publishing Company: Moscow, Russia, 1987.
(3) Coquerel, G. *Chem. Eng. Technol.* **2006**, *29* (2), 182−186.
(4) Coquerel, G. *Enantiomer* **2000**, *5* (5), 481−489.
(5) Kellogg, R. M.; Kaptein, B.; Vries, T. R. *Top. Curr. Chem.* **2007**, *269*, 159−197.
(6) Glikin, A. E.; Sinai, M.Yu. *Zap. VMO (Proc. Russ. Miner. Soc.)* **1983**, *112* (6), 742−748.
(7) Glikin, A. E. *Polymineral-Metasomatic Crystallogenesis*; Springer: New York, 2009.
(8) Jacques, J.; Collet, A.; Wilen, S. H. *Enantiomers, Racemates and Resolutions*; Krieger Publishing Company: Malabar, FL, 1994.
(9) Beckmann, W.; Lorenz, H. *Chem. Eng. Technol.* **2006**, *29* (2), 226−232.
(10) Wermester, N.; Aubin, E.; Pauchet, M.; Coste, S.; Coquerel, G. *Tetrahedron: Asymmetry* **2007**, *18* (7), 821−831.
(11) Kaemmerer, H.; Lorenz, H.; Black, S. N.; Seidel-Morgenstern, A. *Cryst. Growth Des.* **2009**, *9* (4), 1851−1862.
(12) Renou, L.; Morelli, T.; Coste, S.; Petit, M.; Berton, B.; Malandain, J.; Coquerel, G. *Cryst. Growth Des.* **2007**, *7* (9), 1599−1607.
(13) Galland, A.; Dupray, V.; Berton, B.; Morin, S.; Sanselme, M.; Atmani, H.; Coquerel, G. *Cryst. Growth Des.* **2009**, *9* (6), 2713−2718.
(14) Sheldrick, G. M. *SHELX-97, Program for Crystal Structure Refinement*; University of Göttingen: Göttingen, Germany, 1997.
(15) Mullin, J. W. *Crystallization*; Butterworth-Heinemann: Oxford, U.K., 2001.
(16) Scardi, P. In *Powder Diffraction. Theory and Practice*; Dinnebier, R. E., Billingen, S. J. L., Eds.; The Royal Society of Chemistry: Cambridge, U.K., 2008; Chapter 13, pp 377−384.
(17) Treivus, E. B. *Vestnik St. Petersburg State Univ.* **2000**, *7* (1), 83−87.
(18) Sunagawa, I. *Crystals. Growth, Morphology and Perfection*; Cambridge University Press: New York, 2005.